2022 Asia Communications and Photonics Conference (ACP) and International Conference on Information Photonics and Optical Communications (IPOC)

Pairwise Coding for Polarization Multiplexing Turbid UOWC Systems

Bohua Deng[1], Jiwei Wang[2], Zhaoming Wang[1], Chen Chen[2] and H. Y. Fu[1, *]

[1]Tsinghua Shenzhen International Graduate School and Tsinghua-Berkeley Shenzhen Institute
Tsinghua University
Shenzhen, China

[2]School of Microelectronics and Communication Engineering
Chongqing University
Chongqing, China

e-mail: hyfu@sz.tsinghua.edu.cn

2022 Asia Communications and Photonics Conference (ACP) | 978-1-6654-8155-7/22/$31.00 ©2022 IEEE | DOI: 10.1109/ACP55869.2022.10088991

Abstract—**We introduce and experimentally demonstrate a polarization division multiplexing (PDM) based turbid underwater optical wireless communication (UOWC) system with subcarrier pairwise coding (SC-PWC) and subchannel pairwise coding (SCH-PWC) schemes. A sum data rate of 10.4Gbps can be reached by SC-PWC in clear water. And significant BER improvements are achieved by using SC-PWC and SCH-PWC in Maalox simulated varying degrees of turbid ocean water.**

Keywords- underwater optical wireless communication; polarization division multiplexing; pairwise coding

I. INTRODUCTION

Nowadays, people have put forward higher and higher requirements for ocean exploration such as ocean resources detection, marine life protection, and subsea military activities. Underwater optical wireless communication (UOWC), as an essential tool to achieve this goal has recently gained global research interest. Compared with traditional methods, UOWC has relatively low attenuation and has broad bandwidth, thus achieving higher transmission rate. For moderate and clear ocean water, researchers found out that green or blue lasers are optimal choices on account of their low attenuation coefficient [1]. Nevertheless, other researchers later demonstrated that red laser shows better performance in turbid water resulting from low scattering coefficient at longer wavelength [2].

In order to enhance the communication performance of UOWC, researchers mainly focus on increasing the whole system's capacity. Multidimensional multiplexing is a preferable technique to achieve this goal, such as wavelength length multiplexing (WDM) and polarization division multiplexing (PDM). The WDM-PDM transmissions at data rate of 25Gbps using green and blue lasers have been demonstrated in [3]. On the other hand, most UOWC links have frequency selective fading, which is caused by the properties of the light source and detector, or the underwater channel itself. The subcarriers in one orthogonal frequency division multiplexing (OFDM) frame will be degraded differently, which will cause signal-to-noise ratio (SNR) imbalance among those subcarriers. Furthermore, in different ocean types, the presence of chlorophyll, minerals, sediment, and organisms will cause varying degrees of attenuation, including absorption and scattering along the transmission path. Laser's polarization degree can be affected by those suspended particles, and a small amount of circularly polarized light can be converted to linearly polarized light [4]. Therefore, transmission over the same underwater channel will have different effects on two orthogonal polarization light signals. Also, system alignment, turbulence, bubbles, and fish block will introduce SNR difference between two PDM subchannels. In conclusion, the overall communication performance will be limited by SNR imbalance among different subcarriers and between two PDM subchannels.

In this paper, we introduce and experimentally demonstrate two pairwise coding (PWC) techniques to improve the communication performance of a turbid PDM-UOWC system. Subcarrier PWC (SC-PWC) is introduced to solve frequency selective fading problem in pure and low turbidity water. And subchannel PWC (SCH-PWC) is used to mitigate SNR imbalance between two PDM subchannels in highly turbid water. More importantly, these two PWC schemes require only a small amount of additional computation time and complexity, since pairing of symbols is processed together and no feedback is required at the transmitter.

II. PRINCIPLE OF SUB-CARRIER AND SUB-CHANNEL PAIRWISE CODING SCHEMES

A. PWC Encoding

The illustration of PWC encoding and decoding is shown in Fig.1. First, quadrature amplitude modulation (QAM) mapping is applied to two serial input bits, then both QAM symbols rotate a certain angle to increase the minimum distance between symbols. The optimal angle depends on modulation order and SNR imbalance [5], 45° is suitable for most cases. It is assumed that the number of the subcarriers N_d is even and both channels have same descending responses, and the subcarriers in PDM subchannels can be defined as

$$s_{m,n} = [s_{1,1},...,s_{N_d,1},s_{1,2},...,s_{N_d,2}], m \in [1,N_d], n \in [1,2] \quad (1)$$

Thus, the symbols after rotation can be denoted as $s^{\theta} = s_{m,n}e^{j\theta}$. Next in-phase (I) and quadrature (Q) component

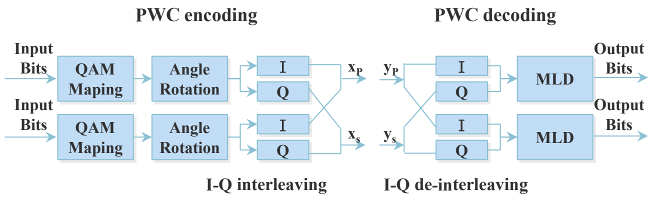

Figure 1. Illustration of PWC encoding and decoding.

interleaving is used to generate the signals for each paired subcarriers or polarization channel.

For SC-PWC, subcarriers with good SNR and bad SNR are paired together in each channel. The p-th pair of subcarriers can be demonstrated as

$$(s_p^{\theta}, s_{N_d-p+1}^{\theta}) = (s_p e^{j\theta}, s_{N_d-p+1} e^{j\theta}), p \in [1, N_d/2] \quad (2)$$

For SCH-PWC, pairwise coding is performed over two PDM subchannels in a similar way. The q-th pair can be demonstrated as

$$(s_{q,1}^{\theta}, s_{q,2}^{\theta}) = (s_{q,1} e^{j\theta}, s_{q,2} e^{j\theta}), q \in N_d \quad (3)$$

The I/Q interleaving is given by

$$\begin{cases} x_{sc} = \Re\left(s_p^{\theta}\right) + j\Re\left(s_{N_d-p+1}^{\theta}\right) \\ y_{sc} = \Im\left(s_p^{\theta}\right) + j\Im\left(s_{N_d-p+1}^{\theta}\right) \end{cases} \begin{cases} x_{sch} = \Re\left(s_{q,1}^{\theta}\right) + j\Re\left(s_{q,2}^{\theta}\right) \\ y_{sch} = \Im\left(s_{q,1}^{\theta}\right) + j\Im\left(s_{q,2}^{\theta}\right) \end{cases}, \quad (4)$$

where $\Re(\bullet)$ and $\Im(\bullet)$ denote the real and imaginary parts of the symbols, x_{sc} and y_{sc} represents two output symbols by SC-PWC, x_{sch} and y_{sch} represents two output symbols by SCH-PWC .

B. PWC Decoding

At the receiver side, the received signal is first rescaled by multiplying the square root of their SNRs, denoted as $x_r^{'}$. Then I-Q de-interleaving is performed based on the interleaving method introduced before. Here, maximum likelihood (MLD) detection is used for symbol decision.

$$D_s = \arg\min_{C_k} \left\{ \left| x_r^{'} - D_k \right|^2 \right\}, \quad (5)$$

$$D_k = \Re\left(C_k e^{j\theta}\right)\sqrt{SNR_{good}} + j\Im\left(C_k e^{j\theta}\right)\sqrt{SNR_{bad}}, \quad (6)$$

where D_k is the rotated and rescaled constellation points, C_k is the constellation alphabet. Finally, bit error rates (BERs) can be calculated after MLD processing.

III. EXPERIMENTAL RESULTS AND DISCUSSIONS

The block diagram of the PDM-UOWC system is shown in Fig.2, where two transmitters and two receivers are utilized to realize PDM. The transmitted bits are mapped to 16-QAM signals and modulated as OFDM signals through the following steps: converting to parallel data, QAM mapping, constellation rotation, interleaving, adding pilot, adding Hermitian symmetry, performing inverse fast Fourier transform (IFFT), adding cyclic prefix (CP), and parallel to serial conversion. The generated signals are then loaded to the arbitrary waveform generator (AWG, AWG7000A, Tektronix) and combined with direct current (DC) components by the bias-tee (ZFBT-6GW+, Mini-circuit). The light sources used as transmitters are vertical cavity surface emitting lasers (VCSELs, DV0680M, DERAY). A peak emission wavelength of 679.6 nm is measured at 10 mA. The laser beams are then combined with a polarization beam splitter (PBS) from two orthogonal orientations perpendicular (s) and parallel (p) directions, and converge into one beam with two polarization states. Then the beam is collimated into parallel light by two plano-convex lens and propagates into the main transmission media: a water tank in dimension of 0.2 m×0.5 m×0.6 m filled with 36L fresh tap water.

The turbidity of the water channel is controlled by different concentration of Maalox, which is commonly used in underwater experiments to simulate different types of ocean water. Its main ingredients are aluminum hydroxide and magnesium hydroxide. The scattering and absorption coefficient of turbid water can be varied by changing the concentration of Maalox in the tank based on reference [6]. The detailed calculated parameters are listed in Tab. 1 [2,7].

At the receiver side, the laser beam is converged by a plano-convex lens and then separated by another PBS, and two avalanche photodiodes (APD, APD210, Menlo Systems, 1 GHz) detect the optical signals and converts them to electrical signals. The outputs of the APDs are captured by two different channels of a real-time oscilloscope (OSC, MSO73304DX, Tektronix) with sampling rate 25 GSa/s. Then the received signals are processed with certain DSP steps in MATLAB 2021a. A vector network analyzer (VNA, N5227A, Agilent, 10 MHz-67 GHz) is used to obtain the frequency of the light source.

The frequency response of the VCSEL shown in Fig. 3(a) is measured by a positive-intrinsic-negative photodetector (Thorlabs PIN, DET025AL) with -3dB modulation band-

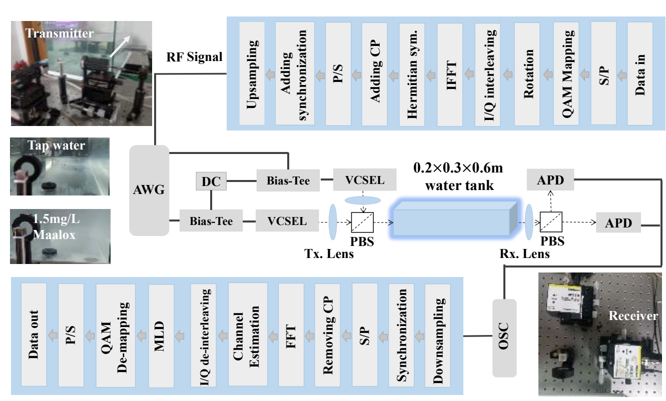

Figure 2. Schematic and experimental setup of the PDM-UOWC System.

TABLE I. OPTICAL ATTENUATION COEFFICIENT FOR FIVE OCEAN WATER TYPES AND CORRESPONDING MAALOX SOLUTION

Water type	Absorption (m^{-1})	Scattering (m^{-1})	Attenuation (m^{-1})	Maalox (mg/L)
Pure sea	0.0472	0.0019	0.0491	0.0950
Clear water	0.1328	0.0290	0.1618	0.2870
Costal	0.2068	0.1700	0.3768	0.6700
Harbor I	0.2107	0.7180	0.9287	1.6600
Harbor II	0.4019	1.4300	1.8319	3.1280

width of 2GHz. The frequency response of the whole system is shown in Fig. 3(b), which reflects that the frequency selective fading may be caused by bandwidth limitation of light source and 1GHz APD. Also, by adding Maalox into water tank, the -6dB bandwidth of polarization p and s decreased from 1.085GHz to 1.050 GHz and 1.075 GHz. This indicates that as suspended particles in the water increases, the frequency response of two channels changed differently. One channel shows a larger fade than the other. This phenomenon resulting from the scattering of these particles affects the polarized light of the two paths differently, thus leading to a larger imbalance between two channels.

Fig 4. (a) plots the calculated BER curves of different PWC schemes in clear water. Since the SNR between two channels is relatively small compared with turbid water, frequency selective fading dominates more than PDM subchannel difference. SC-PWC shows better compensation performance. By using SC-PWC method, the highest rate data is obtained up to 10.4 Gbps under FEC criteria (3.8×10^{-3}). At a BER of 10^{-4}, SC-PWC and SCH-PWC provide a data rate increase of about 1.4 Gbps (18.4%) and about 0.4 Gbps (5.26%) over the uncoded one.

BERs of all data subcarriers under data rate 10.4 Gbps and constellation points of both channels are shown in Fig. 4(b) For uncoded 16QAM signal, the BERs in high index subcarriers are much higher, which is consistent with frequency selective fading problem mentioned before. For SC-PWC, both low and high index subcarriers exist comparable BERs because of interleaving bad SNR subcarriers and good SNR subcarriers. Although low frequency part subcarriers are sacrificed to compensate for

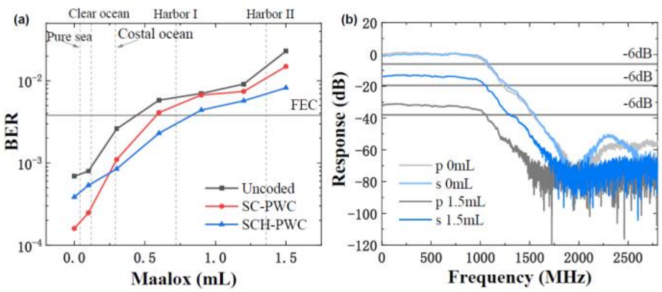

Figure 3. Frequency response of (a) DERAY VCSEL and (b) whole system with 0/1.5mL Maalox.

high frequency subcarriers, the overall BER still get improved by compensation. For SCH-PWC, by interleaving PDM subchannels with good and bad SNR, the BER still appears at high frequencies. However, due to the benefits of constellation rotation and interleaving, the overall BER performance is still better than the uncoded one.

In order to investigate PWC compensation in turbid water, Maalox is used to simulate real ocean water. As shown in Tab. 1, 0.04 mL, 0.12 mL, 0.29 mL, 0.72 mL, 1.36 mL Maalox solution is put into a 36 L water tank to simulate pure sea, clear ocean, coastal ocean, Harbor I and Harbor II water channels, respectively. AWG sampling rate is fixed at 4.8 GSa/s. At Maalox concentration lower than 0.25 mL, mainly for pure sea cand clear ocean, SC-PWC outperforms SCH-PWC. With Maalox concentration increasing, since SNR in each PDM channel begin to decrease, the difference between low index subcarrier and high index subcarrier is no longer significant. Thus, compensation performance of SC-PWC will decrease. In costal ocean, Harbor I and Harbor II, the SCH-PWC outperforms SC-PWC. The increasing scattering of particles amplifies SNR imbalance between two PDM channels. The impact of two PDM channel imbalance dominates compared to frequency selective fading problem. As shown in Fig. 4(c), with a fixed data rate of 9.6 Gbps, SCH-PWC has better robustness in highly turbid water and can achieve the same communication performance facing water with twice the turbidity than uncoded one. Also, after applying SCH-PWC, the designed PDM-UOWC system can support data transmission in Harbor I water.

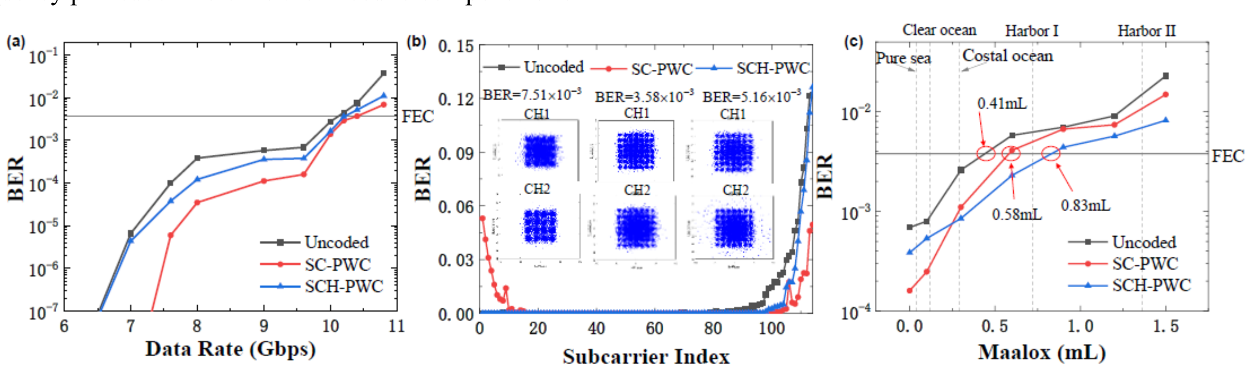

Figure 4. BER of (a) different PWC schemes, (b) different subcarriers at the data rate of 10.4 Gbps, (c) PWC with different Maalox concentrations.

IV. CONCLUSIONS

In this paper, SC-PWC and SCH-PWC schemes are demonstrated for performance improvement of turbid PDM-UWOC systems. By mitigating frequency selective fading, SC-PWC shows better compensation performance in pure sea and clear ocean. The overall data rate can be reached to 10.4 Gbps when using SC-PWC in clear water. Then the Maalox solution is added in the water tank to simulate different turbidity ocean. With the increase of water turbidity， SCH-PWC outperforms SC-PWC in costal ocean, Harbor I and Harbor II. It can achieve the same communication performance facing water with twice the turbidity than uncoded one at BER lower than 3.8×10^{-3}. In conclusion, SC-PWC and SCH-PWC are potential techniques to improve the performance degradation of UWOC links in varying degrees of turbidity water.

ACKNOWLEDGMENT

This work is supported by Shenzhen Technology and Innovation Council (JSGG20210818101404013).

REFERENCES

[1] W. Hou et al., “Undersea narrow-beam optical communications field demonstration, ”Ocean Sensing and Monitoring IX.SPIE, pp. 7-22, 2017.

[2] J. Xu et al., “Underwater wireless transmission of high-speed QAM-OFDM signals using a compact red-light laser, ” Opt Express, vol. 24, no. 8, pp. 8097-109, 2016.

[3] Z. Wang, L. Zhang, Z. Wei, Y. Dong, G. Wei, and H. Fu, “Beyond 25 Gbps OFDM UOWC system based on green and blue laser Diodes with wavelength and polarization multiplexing,” International Conference on Communications and Broadband Networking, 2021.

[4] Y. Zhang, Y. Wang, A. Huang, and X. Hu, “Effect of underwater suspended particles on the transmission characteristics of polarized lasers,” J Opt Soc Am A Opt Image Sci Vis, vol. 36, no. 1, pp. 61-70,201.

[5] J. Boutros and E. Viterbo, “Signal space diversity: a power-and bandwidth-efficient diversity technique for the Rayleigh fading channel,” IEEE Transactions on Information theory, vol. 44, no. 4, pp. 1453-1467, 1998.

[6] A. Laux et al., “The a, b, c s of oceanographic lidar predictions: a significant step toward closing the loop between theory and experiment,” Journal of Modern Optics, vol. 49, no. 3-4, pp. 439-451, 2010.

[7] T. J. Petzold, “Volume scattering functions for selected ocean waters,” Scripps Inst. Oceanography Visibility Lab., San Diego, CA, USA, Tech. Rep. SIO 72–78, pp. 72–78, 1972.